International Journal of Mass Spectrometry 434 (2018) 100–107

Contents lists available at ScienceDirect

International Journal of Mass Spectrometry

journal homepage: www.elsevier.com/locate/ijms

Full Length Article

Differentiation of isomeric methoxychalcones by electrospray ionization tandem mass spectrometry

Xiaoping Zhang[a,*], Jianchuan Liu[a], Jianliang Xiong[b], Yin Ji[a], Yi Zhang[a], Honghan Chen[a], Shuiping Yang[a], Huanwen Chen[a,*]

[a] Jiangxi Key Laboratory for Mass Spectrometry and Instrumentation, East China University of Technology, Nanchang 330013, PR China
[b] School of Pharmaceutical Sciences, Peking University, Beijing 100191, PR China

ARTICLE INFO

Article history:
Received 7 June 2018
Received in revised form 2 September 2018
Accepted 20 September 2018

Keywords:
Methoxychalcone isomers
Differentiation
Electrospray ionization tandem mass spectrometry
Ortho effect

ABSTRACT

Some biological and pharmacological properties of chalcones depend both on the different functional groups and their relative positions. Thus it is important to characterize their structures and to differentiate the isomers. Herein, six positional isomers of methoxychalcone were systematically studied by electrospray ionization tandem mass spectrometry (ESI-MS/MS) in positive ion mode. It was found that the substitution pattern of methoxychalcones changes the ESI-MS/MS fragmentation considerably, especially the *ortho* substituents. The proposed fragmentation mechanisms and interpretation of MS/MS spectral differences for protonated methoxychalcone isomers are supported by density functional theory (DFT) theoretical calculations. Overall, these results indicate that ESI-MS/MS is a very useful technique for distinguishing positional isomers of analogical isomers.

1. Introduction

Chalcones are a group of natural products ubiquitously distributed in the plant kingdom and characterized by the presence of two aromatic rings joining by a three carbon α, β-unsaturated carbonyl skeleton [1]. Chalcones are considered to display a plethora of pharmacological activities, such as antifungal, antimicrobial, anti-inflammatory, antitumor and anticancer properties [2–4]. In addition, chalcones have also been found numerous applications as food additives, photorefractive polymers, and pesticides [5–7]. Since the biological and pharmacological properties of chalcones are greatly depended on the different functional groups and their substituent positions, it is quite significant and challenging to be able to characterize the structures and differentiate the positional isomers.

Currently, several investigations have been carried out on structural characterization and identification of chalcones based on electrospray ionization tandem mass spectrometry (ESI-MS/MS) [8–12]. Pan and co-workers have reported the elimination of a neutral benzene by an intramolecular rearrangement process from protonated chalcone derivatives [11]. George and co-workers have reported that the elimination of ketene takes place in the protonated *ortho*-methoxy chalcone via gas-phase Nazarov cyclization reaction [9]. Still, differentiation and identification structures of positional isomers are one of the greatest challenging analytical issues by using mass spectrometry method because they have exactly the same molecular weight.

ESI-MS/MS has become an indispensable widely used tool for the isomeric differentiation of a wide variety of compounds such as flavonoids, steroids and peptides [13,14]. Some positional isomers can be distinguished by the different fragmentation ions and/or relative abundance differences of the dissociation ions from tandem mass spectra technique under the same conditions [15–17]. Jiang et al have reported the positional effect of the methoxyl substituent, and distinguish three positional isomers of S-methyl methoxylphenylmethylenehydrazine dithiocarboxylates successfully by ESI-MS/MS techniques [18]. Many *ortho* isomers of aromatic compounds can be relatively easily recognized in the ESI mass spectra and electron-impact (EI) mass spectra, due to the so-called "*ortho* effect" [18–25].

In the work presented here, high-resolution ESI-MS/MS was used to investigate the special fragmentation behaviors and the differentiation of six methoxychalcone isomers (Scheme 1). The possible fragmentation mechanisms and interpretation of MS/MS spectral differences for protonated methoxychalcone isomers were demonstrated by density functional theory (DFT) theoretical calculations. Our results present interesting and valuable data and reliable information for the further rapid identification of similar types of chalcones in plant or medicine extracts.

* Corresponding authors.
E-mail addresses: zhangxpsunshine@163.com (X. Zhang), chw8868@gmail.com (H. Chen).

https://doi.org/10.1016/j.ijms.2018.09.023
1387-3806/

Chalcones

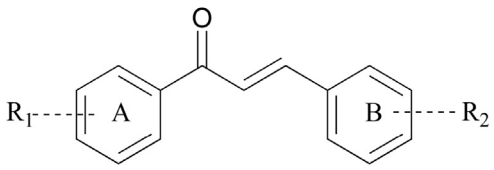

	Mw	R_1	R_2
1	238	*o*-OMe	H
2	238	*m*-OMe	H
3	238	*p*-OMe	H
4	238	H	*o*-OMe
5	238	H	*m*-OMe
6	238	H	*p*-OMe

Scheme 1. Structures of the studied compounds **1**–**6**.

2. Experimental details

Methanol HPLC grade were purchased from Sigma-Aldrich (St. Louis, MO, USA) and ultrapure water (Milli-Q) from Millipore System (Bedford, USA). The chalcone isomers with a OCH_3 substituent either on the A ring (*o*-, *m*-, *p*-) or B ring (*o*-, *m*-, *p*-) are listed in Scheme 1. These compounds were gifted by Xu's group from Hangzhou Normal University [26].

The ESI experiments, both MS and low-energy collision induced dissociation (CID), were performed on a micrOTOF QII (Q-TOF) mass spectrometer (Bruker Company, USA), equipped with an ESI ion source. The diluted solvent was directly infused into the electrospray ionization source of the mass spectrometer with a syringe pump at a flow-rate of 3 μL/min. Parameters for analysis were set as follows: capillary voltage, 3.5 kV; drying gas temperature, 180 °C; drying gas flow, 2 l/min and nebulizer gas pressure, 0.4 bar (both were N_2). In MS/MS experiments, mass width of the selected ion was 1.0 Da, and collision energy of CID for the selected ions was set at the range of 2 eV–20 eV with argon as the collision gas. The accurate mass data of the molecular ions were provided by the newest software Data Analysis 4.0 (Bruker Daltonics, Bremen, Germany), which obtained a list of possible elemental formula by using the Smart Formula Editor.

Theoretical calculations were performed using the Gaussian 09 program [27]. The geometries of the target species were optimized using the DFT method at the B3LYP/6-311+G(d,p) level. The optimized structures were identified as a true minimum in energy by the absence of imaginary frequencies. Vibrational frequencies of all the key species were calculated at the same level of theory. The energies discussed here are the sum of electronic and thermal free energy.

3. Results and discussion

Chalcone isomers **1** – **6** (Scheme 1) are easily protonated due to their carbonyl structures reported by other authors [11,28]. Fig. 1 shows the CID mass spectra of six protonated chalcone isomers under the same conditions. In the CID mass spectra of the $[M+H]^+$ ions of the chalcone isomers studied, many of the fragment ions can be classified as A or B ring, meaning that these product ions remain one ring portion while the other ring lost. A comparison of these spectra shows that the isomers can be easily distinguished from each other based on the collision ionization characteristic ions and different intensities of small molecule eliminations, e.g. elimination of styrene (route 1), elimination of A-ring (route 2), elimination of B-ring (route 3), and elimination of ketene (route 4). The main product ions observed in each MS/MS spectrum are summarized in Table 1, and the corresponding fragmentation behaviors will be discussed in further detail below.

3.1. Fragmentation of isomeric chalcones

Under low-energy CID conditions, the elimination of styrene to form the ion at *m/z* 135 dominates the spectrum, with a minor elimination of CH_3 radical also being observed (Fig. 1a, Scheme 1). As shown in Fig. 1b, the low-energy CID spectrum of $[\mathbf{2} + H]^+$ is quite different from those of $[\mathbf{1} + H]^+$. The main fragmentation pathway of $[\mathbf{2} + H]^+$ is elimination of anisole (A-ring) to form ion at *m/z* 131 (100%), which undergoes a further loss of CO to form ion at *m/z* 103. In addition, a minor fragment ion at *m/z* 161 is formed as a result of the elimination of benzene (B-ring). It should be noted that the relative intensity of ion generating via the loss of styrene is very small (7%) for $[\mathbf{2} + H]^+$, which is in stark contrast to that of $[\mathbf{1} + H]^+$. In a similar behavior to $[\mathbf{2} + H]^+$, the main product ion for $[\mathbf{3} + H]^+$ also generates via the elimination of anisole (A-ring) to yield the ion at *m/z* 131 (65%). Other fragmentation pathways observed containing an abundant loss of styrene (containing the B-ring) to form the ion at *m/z* 135 (36%), together with a minor loss of benzene (B-ring) to yield *m/z* 161 (9%). The possible fragmentation pathways of $[\mathbf{1} + H]^+$, $[\mathbf{2} + H]^+$, and $[\mathbf{3} + H]^+$ are depicted in Schemes 2–4, respectively.

From Fig. 2d, upon collisional activation the ESI-generated $[\mathbf{4} + H]^+$ ion mainly exhibits three fragment ions at *m/z* 197 (100%), *m/z* 105 (30%) and *m/z* 91 (40%), as well as other minor product ions listed in Table 1. Accurate mass measurement reveals that the fragment ion at *m/z* 197.0959 has the formula $C_{14}H_{13}O$, which resulted from of the loss of C_2H_4O (ketene) from precursor ion at *m/z* 239. The methoxyl (on the B-ring) facilitates a Nazarov cyclization to the corresponding protonated 3-aryl-indanones then undergoes an elimination of ketene, as previously reported [9]. The fragment ion of *m/z* 105 (30%) is attributed to the benzoyl cation, originating from the *o*-methoxy styrene elimination of the parent ion. The fragment ion *m/z* 91 (40%) is attributed to the benzyl, which may also be an interesting ion. The possible fragmentation pathways of $[\mathbf{4} + H]^+$ is depicted in Scheme 5. In Fig. 2e and f, the major fragment ions are *m/z* 161 and *m/z* 131 due to the elimination of benzene (A-ring) and anisole (B-ring), respectively. However, the fragment ions (*m/z* 197) resulting from elimination of ketene are extremely lower in abundance than that from $[\mathbf{4} + H]^+$. In addition, the intensity of *m/z* 131 is higher than that of *m/z* 161 from $[\mathbf{5} + H]^+$, which is contrary to those from $[\mathbf{6} + H]^+$. The possible fragmentation pathways of $[\mathbf{5} + H]^+$ and $[\mathbf{6} + H]^+$ are depicted in Schemes 6 and 7, respectively. As a result, the six methoxychalcone isomers can be differentiated solely by tandem MS. Due to the "*ortho* effect", several structural diagnostic product ions at *m/z* 135 and *m/z* 197 are detected in the CID of the ortho isomers **1** and **4**, respectively.

3.2. Breakdown curves

Evaluation of breakdown curves can offer more information on different fragmentation mechanisms such as differentiation between consecutive and competitive fragmentation pathways, the identification of tautomers and isomers, the stability of fragment ions, and the relationship between the selected ions and the collision energy [8,18]. The breakdown curves plotted in Fig. 2 show how the relative intensities of fragment ions generated by CID mass

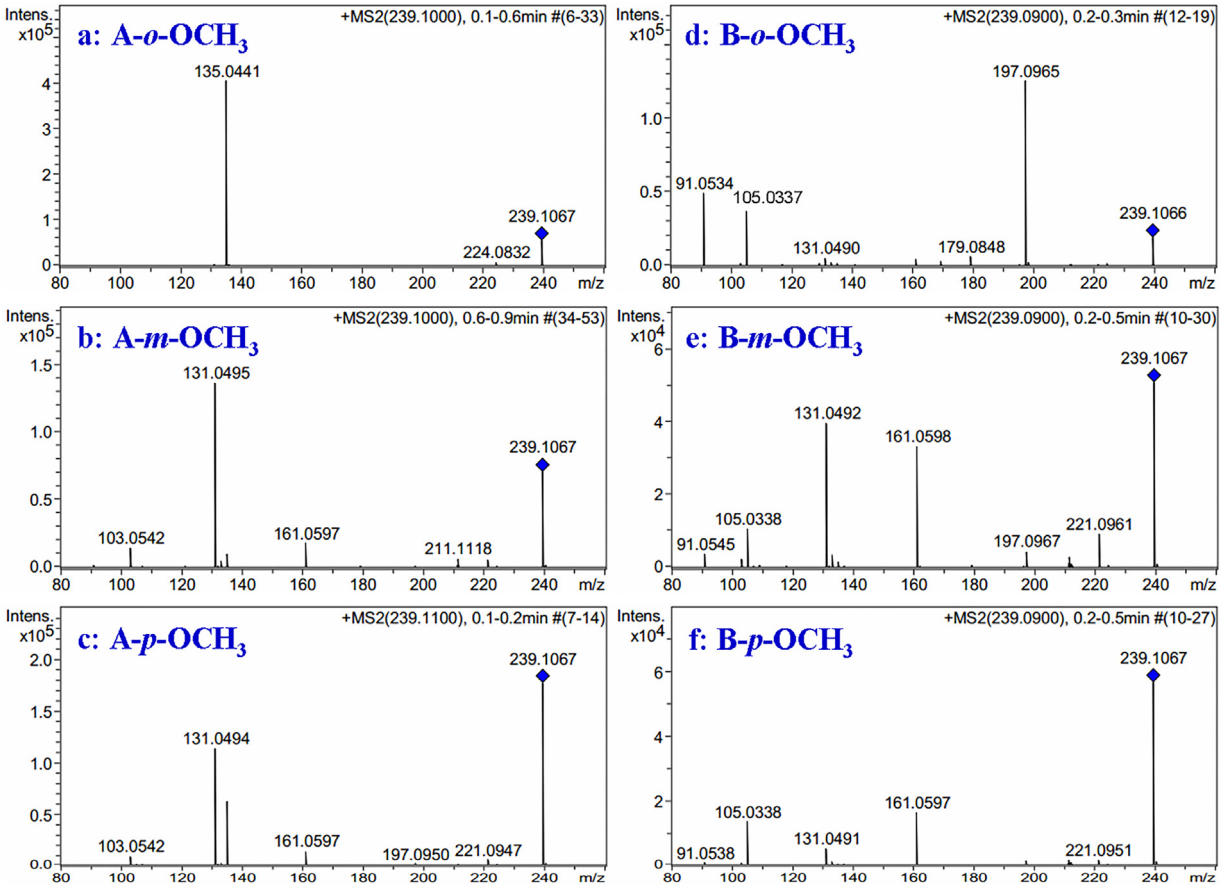

Fig. 1. The CID mass spectra of protonated chalcone isomers (**1** – **6**) by ESI-Q/TOF with the collision energy at 12 eV. (a) A-*o*-OCH_3 chalcone, (b) A-*m*-OCH_3 chalcone, (c) A-*p*-OCH_3 chalcone, (d) B-*o*-OCH_3 chalcone, (e) B-*m*-OCH_3 chalcone, (f) B-*p*-OCH_3 chalcone.

Table 1
The CID mass spectra of ESI-produced $[M+H]^+$ of chalcone isomers.

Fragment ions	Elemental composition	1	2	3	4	5	6
P[a]	$C_{16}H_{15}O_2^+$	239(14)	239(52)	239(100)	239(15)	239(100)	239(100)
P – CH_3	$C_{15}H_{12}O_2^+$	224(2)	–	224(2)	224(1)	224(1)	–
P – H_2O	$C_{16}H_{13}O^+$	–	221(4)	221(5)	–	221(18)	221(3)
P – C_2H_2O	$C_{14}H_{13}O^+$	–	–	197(2)	197(100)	197(9)	197(3)
P – benzene	$C_{10}H_9O_2^+$	–	161(13)	161(9)	161(3)	161(65)	161(29)
P – styrene	$C_8H_7O_2^+$	135(100)	135(7)	135(36)	135(1)	135(3)	–
P –benzaldehyde	$C_9H_9O^+$	–	133(3)	–	133(2)	133(7)	133(2)
P – anisole	$C_9H_7O^+$	–	131(100)	131(65)	131(4)	131(78)	131(11)
Benzoyl cation	$C_7H_5O^+$	–	–	–	105(30)	105(21)	105(24)
Styrene cation	$C_8H_7^+$	–	103(10)	103(6)	–	103(5)	–
Benzyl	$C_7H_7^+$	–	–	–	91(40)	91(7)	91(1)
Other	$C_{14}H_{11}^+$	–	–	–	179(5)	179(1)	–

[a] P = $[M+H]^+$, parent ions.

spectra of $[M + H]^+$ ions of compounds **1** – **6** varied as the collision energies ranging from 2 to 20 eV. The *ortho* isomers (**1** and **4**) require very little collisional activation to undergo fragmentation than *m*eta and *para* ones (**2**, **3**, **5**, and **6**). For example, the CID spectrum of $[\mathbf{1} + H]^+$ shows an intense peak at *m/z* 135, due to a loss of styrene, which is distinct even at a collision energy value as low as 6 eV (Fig. 2a). Since the *m/z* 239 ion from *meta* and *para* isomers require more energy to initiate decomposition (Fig. 2b, c, e, and f). The reason is attributed to a charge-mediated "*ortho* effect". In addition, the spectra of the six isomers are apparently different from each other.

The differences in the fragmentation of the isomeric series of *ortho*-, *meta*-, and *para*-substituted chalcones have been expressed quantitatively by comparing the calculated values of the coefficients μ [29]. For all the compounds investigated, Table 2 presents the ratios of the relative abundances of the fragment ions to the corresponding precursor ion or fragment ion, e.g., $\mu_1 = I_{131}/I_{239}$. As can be seen from the data in Table 2, the differences between the relative abundances of the peaks of the selected fragment ions and its

Table 2
Values of μ_1 – μ_5 calculated from ESI tandem mass spectra of **1** – **6**.

Compounds	μ_1	μ_2	μ_3	μ_4	μ_5
C1	–	7.14	–	–	–
C2	1.92	0.13	0.25	–	0.52
C3	0.65	0.36	0.09	0.02	18
C4	0.26	0.07	0.2	6.67	0.35
C5	0.78	0.03	0.65	0.09	0.05
C6	0.11	–	0.29	0.03	–

$\mu_1 = I_{131}/I_{239}$, $\mu_2 = I_{135}/I_{239}$, $\mu_3 = I_{161}/I_{239}$, $\mu_4 = I_{197}/I_{239}$, $\mu_5 = I_{135}/I_{161}$.

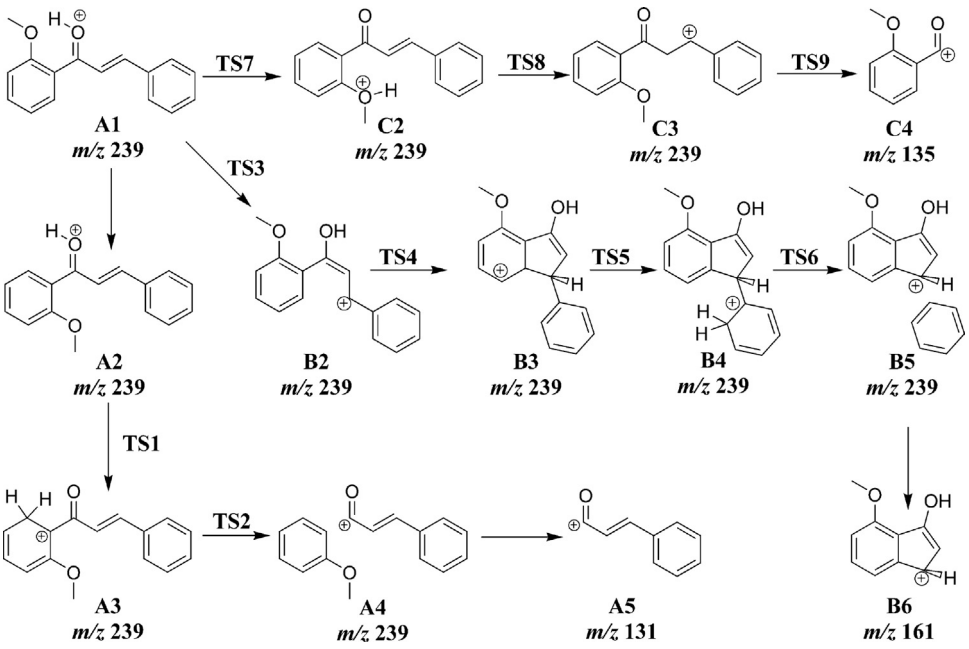

Scheme 2. Proposed reaction pathways for the fragmentation of [**1** + H]$^+$.

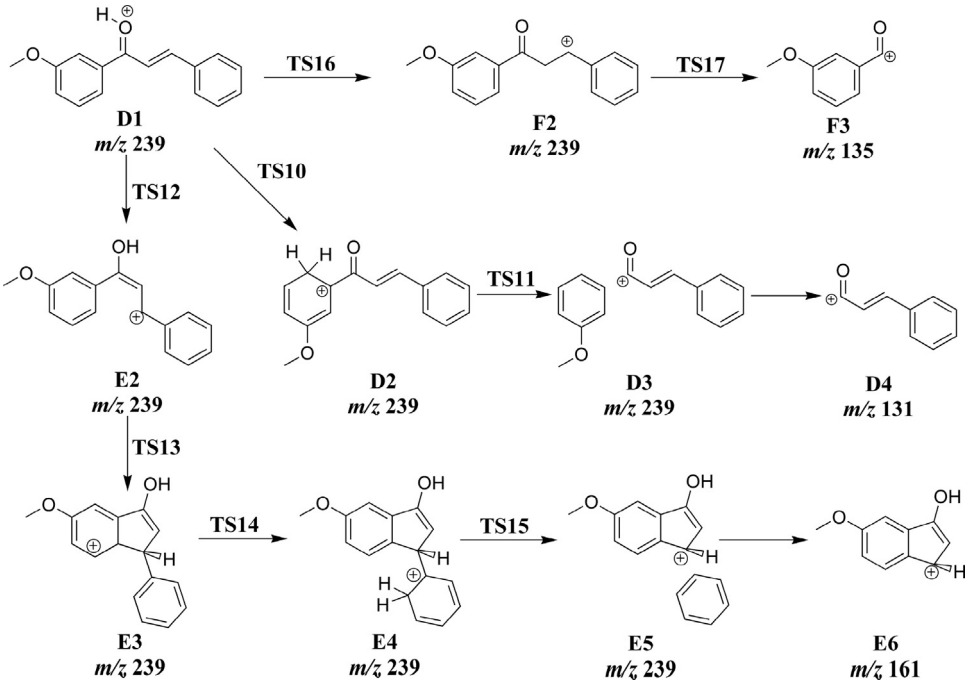

Scheme 3. Proposed reaction pathways for the fragmentation of [**2** + H]$^+$.

precursor ions may be sufficient to differentiate between particular isomers of substituted chalcones. It is possible to use the values of coefficients μ for differentiation of the position of the substitution of the OCH_3 group.

3.3. Mechanisms of positional factors and theoretical calculations

To provide insight into the remarkable fragmentation differences among compounds 1–6, DFT calculations were carried out at the B3LYP/6-31+G(d,p) level of theory. Calculations reveal that the most thermodynamically favorable protonation site is carbonyl oxygen. During the subsequent fragmentation process, the external proton has to transfer to other less favored sites. Schematic potential energy surface scans for the dissociation of [**M** + H]$^+$ is shown in Fig. 3.

From the calculation results of Fig. 3(a), it can be found that the energy barriers in route 2 (blue line) and route 3 (rose red line) are both significantly higher than that in route 1 (green line). In route 1, the proton in carboy oxygen of **A1** can occur two steps 1,5-proton migration to form **C3**, then dissociation to form ion *m/z* 135 (Scheme 2). Thus, the ion *m/z* 135 is the base peak, which is in good agreement with the CID experimental results (Fig. 1a). In Fig. 3(b), the energy barriers of eliminations of A-ring (blue line, route 2), B-ring (rose red line, route 3) and styrene (green line, route 1), follows the order: 212.2 kJ/mol (elimination of A-ring) <226.0 kJ/mol (elimination of styrene) ≈226.7 kJ/mol (elimination of B-ring). The sum

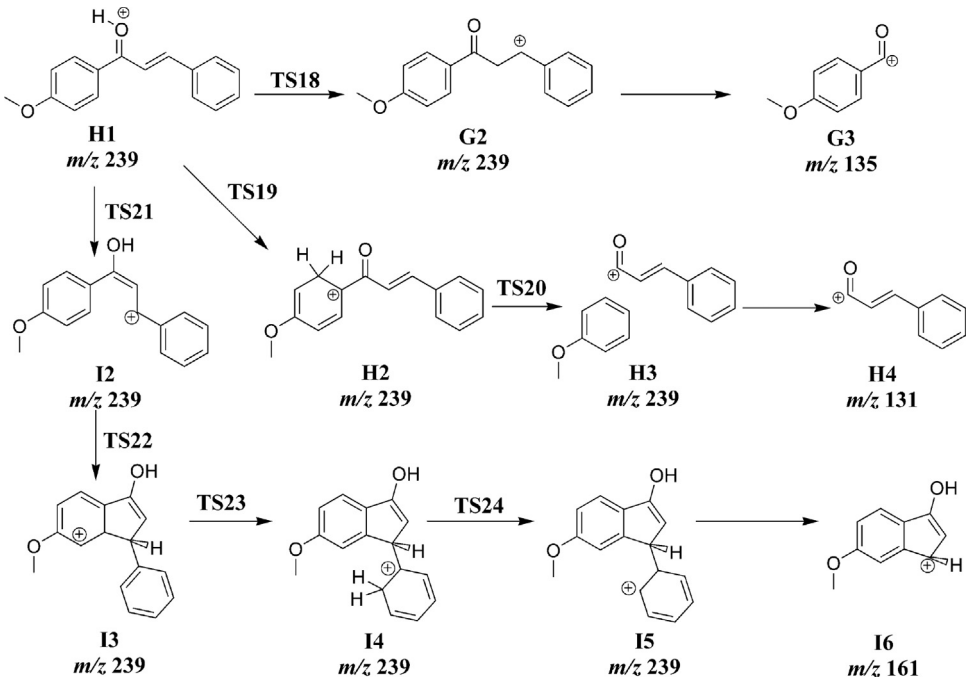

Scheme 4. Proposed reaction pathways for the fragmentation of [**3** + H]$^+$.

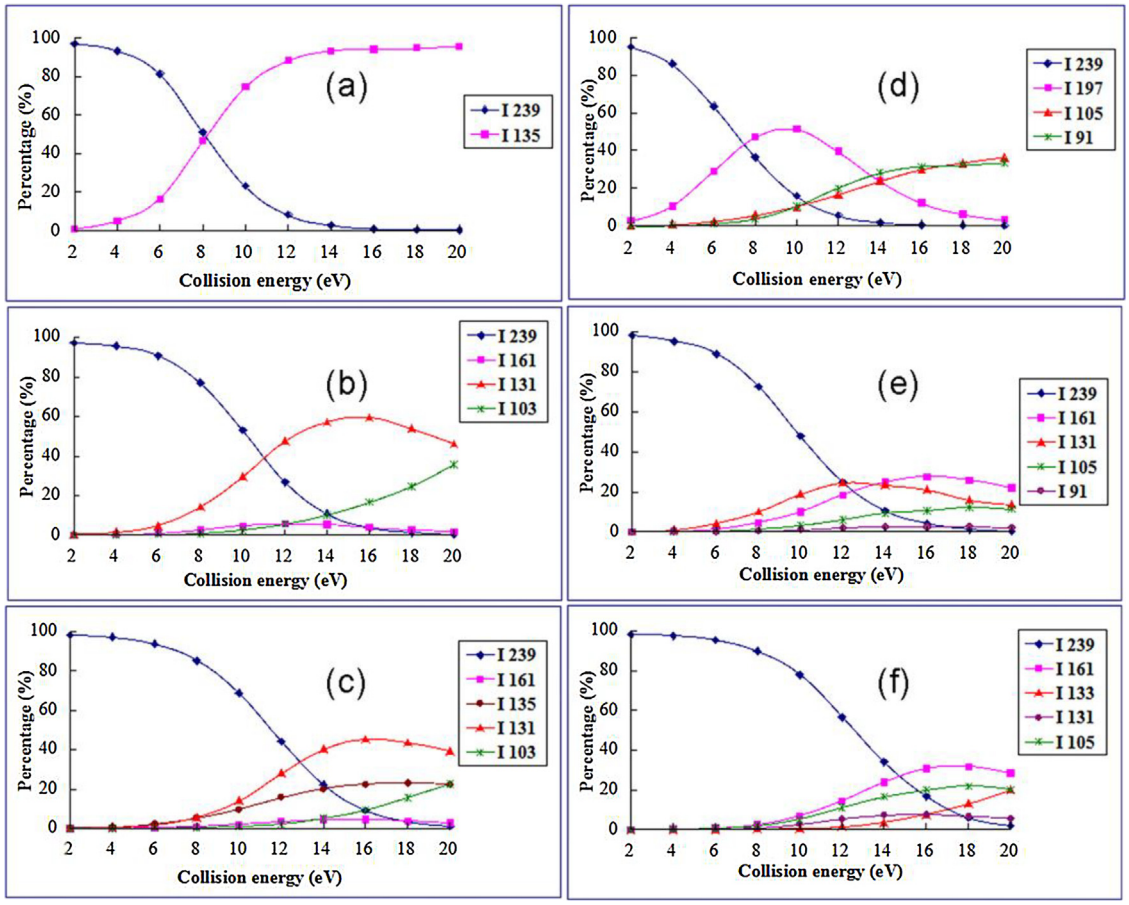

Fig. 2. The energy-resolved plot for protonated chalcones. (a) A-*o*-OCH_3 chalcone, (b) A-*m*-OCH_3 chalcone, (c) A-*p*-OCH_3 chalcone, (d) B-*o*-OCH_3 chalcone, (e) B-*m*-OCH_3 chalcone, (f) B-*p*-OCH_3 chalcone.

free energy of **E6** and B-ring (benzene) is 57 kJ/mol less than that of **F3** and styrene. In Fig. 3(c), the energy barriers of eliminations of A-ring, B-ring and styrene, follows the order: 199.8 kJ/mol (elimination of A-ring) < 205.6 kJ/mol (elimination of styrene) <251.4 kJ/mol (elimination of B-ring). Considering the results of dynamics and thermodynamics, the intensities of these three ions should follows

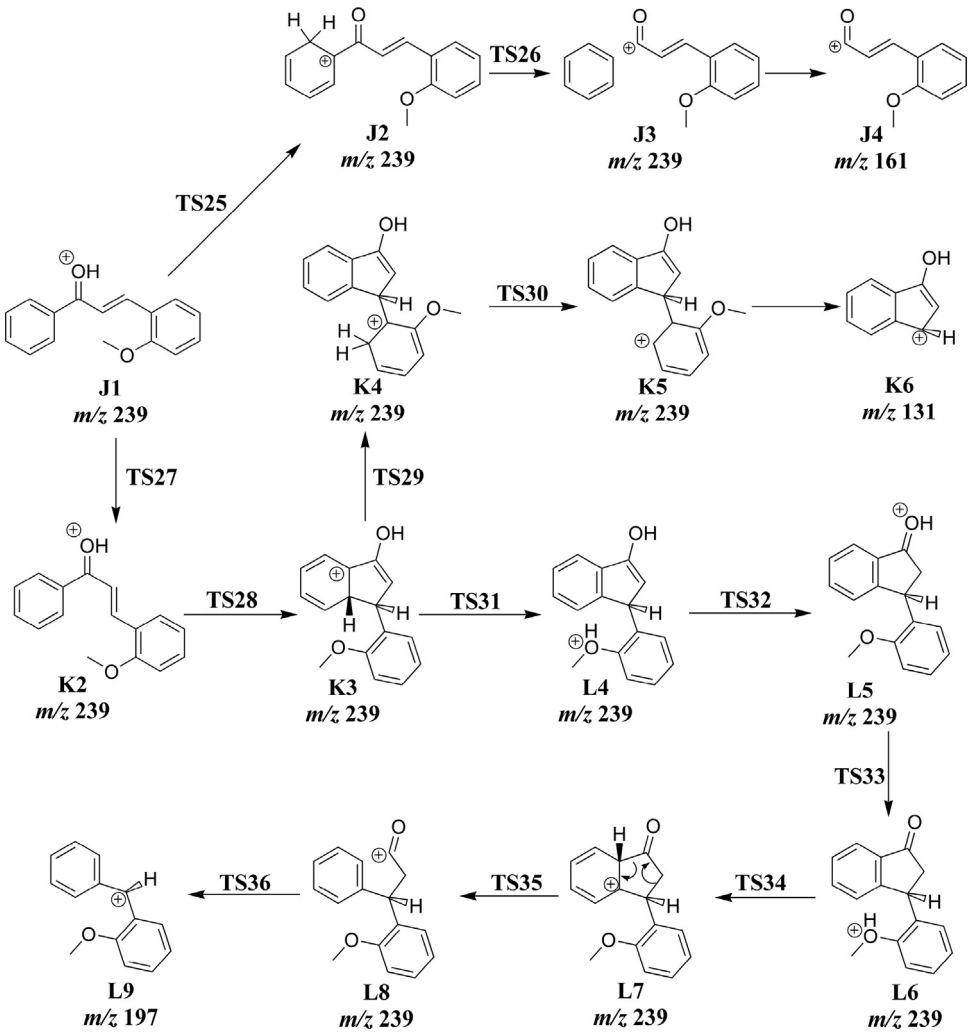

Scheme 5. Proposed reaction pathways for the fragmentation of [**4** + H]$^+$.

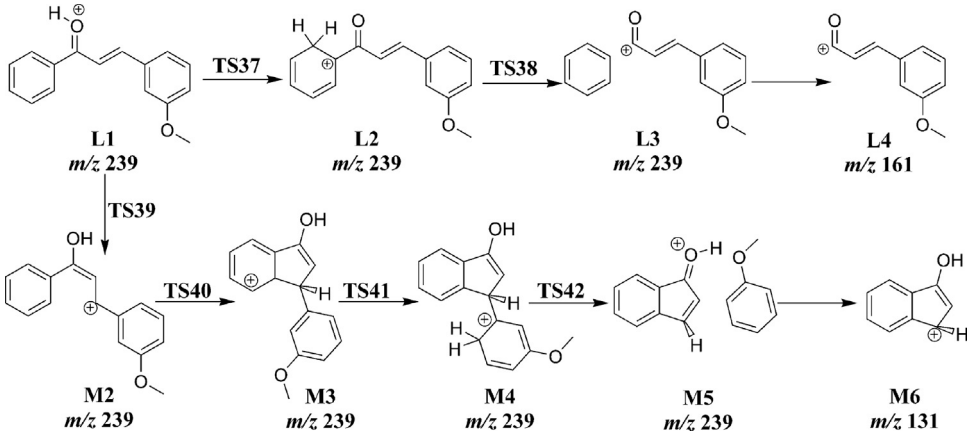

Scheme 6. Proposed reaction pathways for the fragmentation of [**5** + H]$^+$.

the order: *m/z* 131 >*m/z* 161 > *m/z* 135 (A-*m*-OCH_3 chalcone), *m/z* 131 > *m/z* 135 > *m/z* 161 (A-*p*-OCH_3 chalcone), respectively, which are in good agreement with the CID results (Fig. 1b and c).

In a similar way, as shown in Fig. 3(d), the energy barriers in route 2 (blue line) and route 3 (rose red line) are both significantly higher than that in route 4 (red line). In route 4, due to the *ortho*-effect of OCH_3 group, **J1** facilitates a Nazarov cyclization to the corresponding protonated 3-aryl-indanones (**K3**) by mediating a critical proton transfer. Then continue to undergo many steps proton transport catalysis facilitated by the same *ortho* OCH_3 group producing intermediates that eliminate ketene to yield ion *m/z* 197 (Scheme 5). Thus, the ion *m/z* 197 is the base peak, which is in good agreement with the CID experimental results (Fig. 1d). In Fig. 3(e) and (f), the energy barriers of eliminations of A-ring (blue line, route 2) and B-ring (rose red line, route 3), follows the order: 229.7 kJ/mol (elimination of B-ring) <230.7 kJ/mol (elimination of

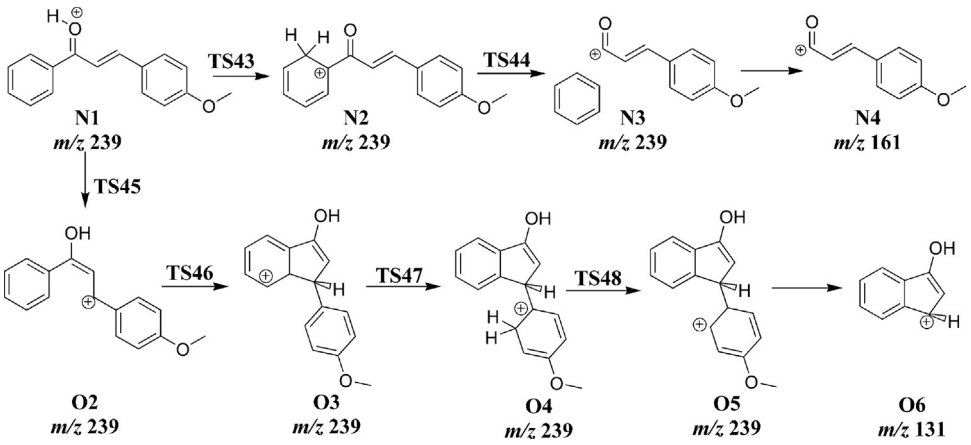

Scheme 7. Proposed reaction pathways for the fragmentation of [**6** + H]$^+$.

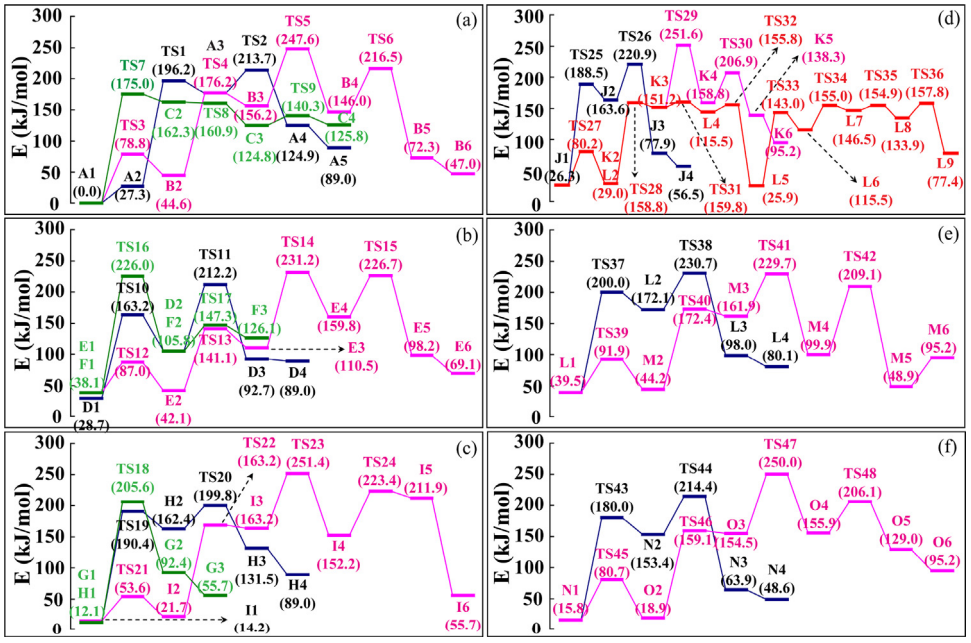

Fig. 3. Potential energy diagram for [**M** + H]$^+$. (a) A-*o*-OCH_3 chalcone, (b) A-*m*-OCH_3 chalcone, (c) A-*p*-OCH_3 chalcone, (d) B-*o*-OCH_3 chalcone, (e) B-*m*-OCH_3 chalcone, (f) B-*p*-OCH_3 chalcone. The green line shows the elimination of styrene, the blue line shows the elimination of A ring, the rose red shows the elimination of B ring, and the red line shows the elimination of ketene.

A-ring), 250.0 kJ/mol (elimination of B-ring) >214.4 kJ/mol (elimination of A-ring), respectively. Thus, the intensity of *m/z* 131 is higher than that of *m/z* 161 in B-*m*-OCH_3 chalcone, while the intensity of *m/z* 131 is lower than that of *m/z* 161 in B-*p*-OCH_3 chalcone, which are in good agreement with the CID results (Fig. 1e and f).

4. Conclusion

In this paper, the *ortho*, *meta* or *para* positional isomers of six OCH_3-substituted isomeric chalcones have been investigated by ESI-MS/MS. Four main fragmentation reactions, elimination of A-ring, B-ring, styrene, and ketene were observed in the CID-MS spectra. Due to the "*ortho* effect", the *o*-isomers A-*o*-OCH_3 chalcone and B-*o*-OCH_3 have been found to undergo styrene elimination and ketene elimination, respectively, to afford several structurally diagnostic product ions. Also, distinctive differences of A-ring elimination and B-ring elimination were observed in the tandem MS spectra of the *meta*- and *para*- isomers. Thereby, the significant difference in the relative abundance of the fragment ions, indicating that these six positional isomers were differentiated solely by tandem MS. Moreover, these results provide basic information to develop a general MS-based method that can be used to differentiate isomers with subtle structural differences.

Acknowledgments

The authors are greatly indebted to Professor Kezhi Jiang and Professor Liwen Xu at Hangzhou Normal University for their invaluable assistance. This work was supported by the National Natural Science Foundation of China (No. 21465002), Science and Technology Planning Project at the Ministry of Science and Technology of Jiangxi Province (No. 20165BCB19013), the Jiangxi Key Laboratory for Mass Spectrometry and Instrumentation Open Foundation (JXMS201707), and the Research Fund of East China University of Technology (No. DHBK2016131).

Appendix A. Supplementary data

Supplementary material related to this article can be found, in the online version, at doi:https://doi.org/10.1016/j.ijms.2018.09.023.

References

[1] F.A. Tomás-Barberán, M.N. Clifford, Flavanones, chalcones and dihydrochalcones – nature, occurrence and dietary burden, J. Sci. Food Agric. 80 (2000) 1073–1080.

[2] H.K. Hsieh, L.T. Tsao, J.P. Wang, C.N. Lin, Synthesis and anti-inflammatory effect of chalcones, J. Pharm. Pharmacol. 52 (2000) 163–171.

[3] S.N. López, M.V. Castelli, S.A. Zacchino, J.N. Domínguez, G. Lobo, J. Charris-Charris, J.C.G. Cortés, J.C. Ribas, C. Devia, A.M. Rodríguez, R.D. Enriz, In vitro antifungal evaluation and structure–activity relationships of a new series of chalcone derivatives and synthetic analogues, with inhibitory properties against polymers of the fungal cell wall, Bioorg. Med. Chem. 9 (2001) 1999–2013.

[4] R. De Vincenzo, C. Ferlini, M. Distefano, C. Gaggini, A. Riva, E. Bombardelli, P. Morazzoni, P. Valenti, F. Belluti, F.O. Ranelletti, S. Mancuso, G. Scambia, In vitro evaluation of newly developed chalcone analogues in human cancer cells, Cancer Chemoth. Pharm. 46 (2000) 305–312.

[5] S. Maqsood, S. Benjakul, F. Shahidi, Emerging role of phenolic compounds as natural food additives in fish and fish products, Crit. Rev. Food Sci. 53 (2013) 162–179.

[6] T.A. Fayed, A novel chalcone-analogue as an optical sensor based on ground and excited states intramolecular charge transfer: a combined experimental and theoretical study, Chem. Phys. 324 (2006) 631–638.

[7] Q. Xu, Z. Yang, D. Yin, F. Zhang, Synthesis of chalcones catalyzed by a novel solid sulfonic acid from bamboo, Catal. Commun. 9 (2008) 1579–1582.

[8] Y. Tai, S. Pei, J. Wan, X. Cao, Y. Pan, Fragmentation study of protonated chalcones by atmospheric pressure chemical ionization and tandem mass spectrometry, Rapid Commun. Mass Spectrom. 20 (2006) 994–1000.

[9] M. George, V.S. Sebastian, P.N. Reddy, R. Srinivas, D. Giblin, M.L. Gross, Gas-phase Nazarov cyclization of protonated 2-methoxy and 2-hydroxychalcone: an example of intramolecular proton-transport catalysis, J. Am. Soc. Mass Spectrom. 20 (2009) 805–818.

[10] J. Cyriac, J. Paulose, M. George, M. Ramesh, R. Srinivas, D. Giblin, M.L. Gross, The role of methoxy group in the Nazarov cyclization of 1,5-bis-(2-methoxyphenyl)-1,4-pentadien-3-one in the gas phase and condensed phase, J. Am. Soc. Mass Spectrom. 25 (2014) 398–409.

[11] N. Hu, Y.-P. Tu, K. Jiang, Y. Pan, Intramolecular charge transfer in the gas phase: fragmentation of protonated sulfonamides in mass spectrometry, J. Org. Chem. 75 (2010) 4244–4250.

[12] J. Zhang, J.S. Brodbelt, Structural characterization and isomer differentiation of chalcones by electrospray ionization tandem mass spectrometry, J. Mass Spectrom. 38 (2003) 555–572.

[13] V. Vukics, A. Guttman, Structural characterization of flavonoid glycosides by multi-stage mass spectrometry, Mass Spectrom. Rev. 29 (2010) 1–16.

[14] G. Hopfgartner, E. Bourgogne, Quantitative high-throughput analysis of drugs in biological matrices by mass spectrometry, Mass Spectrom. Rev. 22 (2003) 195–214.

[15] X. Zhang, F. Li, H. Lv, Y. Wu, G. Bian, K. Jiang, On the origin of the methyl radical loss from deprotonated ferulic and isoferulic acids: electronic excitation of a transient structure, J. Am. Soc. Mass Spectrom. 24 (2013) 941–948.

[16] K.B. Herath, C.S. Weisbecker, S.B. Singh, A.B. Attygalle, Circumambulatory movement of negative charge ("ring walk") during gas-phase dissociation of 2,3,4-trimethoxybenzoate anion, J. Org. Chem. 79 (2014) 4378–4389.

[17] A.B. Attygalle, J.B. Bialecki, U. Nishshanka, C.S. Weisbecker, J. Ruzicka, Loss of benzene to generate an enolate anion by a site-specific double-hydrogen transfer during CID fragmentation of *o*-alkyl ethers of *ortho*-hydroxybenzoic acids, J. Mass Spectrom. 43 (2008) 1224–1234.

[18] K. Jiang, G. Bian, Y. Pan, G. Lai, Recognizing *ortho*-, *meta*- or *para*-positional isomers of S-methyl methoxylphenylmethylenehydrazine dithiocarboxylates by ESI-MS^2: the positional effect of the methoxyl substituent, Int. J. Mass Spectrom. 299 (2011) 13–19.

[19] J.G. Smith, G.L. Wilson, J.M. Miller, Mass spectra of some isopropyl benzene derivatives. A study of the *ortho* effect, Org. Mass Spectrom. 10 (1975) 5–17.

[20] S. Tajima, T. Azami, H. Shizuka, T. Tsuchiya, An investigation of the mechanism of single and double hydrogen atom transfer reactions in alkyl benzoates by the *ortho* effect, Org. Mass Spectrom. 14 (1979) 499–502.

[21] D. Błachut, W. Danikiewicz, M. Olejnik, Z. Czarnocki, Electron ionization mass spectrometry as a tool for the investigation of the ortho effect in fragmentation of some Schiff bases derived from amphetamine analogs, J. Mass Spectrom. 39 (2004) 966–972.

[22] P. Nagi Reddy, R. Srikanth, N. Venkateswarlu, R. Nageswara Rao, R. Srinivas, Electrospray ionization tandem mass spectrometric study of three isomeric substituted aromatic sulfonic acids; differentiation via ortho effects, Rapid Commun. Mass Spectrom. 19 (2005) 72–76.

[23] A. Attygalle, J. Ruzicka, D. Varughese, J. Sayed, An unprecedented *ortho* effect in mass spectrometric fragmentation of even-electron negative ions from hydroxyphenyl carbaldehydes and ketones, Tetrahedron Lett. 47 (2006) 4601–4603.

[24] S.W. Holman, P. Wright, G.J. Langley, High-throughput approaches towards the definitive identification of pharmaceutical drug metabolites. 1. Evidence for an ortho effect on the fragmentation of 4-benzenesulfinyl-3-methylphenylamine using electrospray ionisation mass spectrometry, Rapid Commun. Mass Spectrom. 22 (2008) 2355–2365.

[25] F.B. Jariwala, M. Figus, A.B. Attygalle, *Ortho* effect in electron ionization mass spectrometry of N-acylanilines bearing a proximal halo substituent, J. Am. Soc. Mass Spectrom. 19 (2008) 1114–1118.

[26] F. Ye, Z.-J. Zheng, L. Li, K.-F. Yang, C.-G. Xia, L.-W. Xu, Development of a novel multifunctional N,P ligand for highly enantioselective palladium-catalyzed asymmetric allylic etherification of alcohols and silanols, Chem. Eur. J. 19 (2013) 15452–15457.

[27] M. Frisch, G.W. Trucks, H.B. Schlegel, G.E. Scuseria, M.A. Robb, J.R. Cheeseman, V.G. Zakrzewski, J.A. Montgomery, R.E.S. Jr, J.C. Burant, S. Dapprich, J.M. Millam, A.D. Daniels, K.N. Kudin, M.C. Strain, O. Farkas, J. Tomasi, V. Barone, M. Cossi, R. Cammi, B. Mennucci, C. Pomelli, C. Adamo, S. Clifford, J. Ochterski, G.A. Petersson, P.Y. Ayala, Q. Cui, K. Morokuma, D.K. Malick, A.D. Rabuck, K. Raghavachari, J.B. Foresman, J. Cioslowski, J.V. Ortiz, B.B. Stefanov, G. Liu, A. Liashenko, P. Piskorz, I. Komaromi, R. Gomperts, R.L. Martin, D.J. Fox, T. Keith, M.A. Al-Laham, C.Y. Peng, A. Nanayakkara, C. Gonzalez, M. Challacombe, P.M.W. Gill, B. Johnson, W. Chen, M.W. Wong, J.L. Andres, C. Gonzalez, M.E. Head-Gordon, S. Replogle, J.A. Pople, Gaussian 03, Revision B.03, Gaussian, Inc., Wallingford, CT, 2004.

[28] Y.-P. Tu, Dissociative protonation sites: reactive centers in protonated molecules leading to fragmentation in mass spectrometry, J. Org. Chem. 71 (2006) 5482–5488.

[29] N. Zdzisława, Structural assignment of chalcones and differentiation of their isomeric derivatives by electron ionization induced fragmentation, Rapid Commun. Mass Spectrom. 18 (2004) 2513–2516.